Neurogenesis-induced forgetting is associated with reduced neuronal activity in CA1 during context fear memory retrieval

Alexandria Evans[1], Gavin A. Scott[1] & Jonathan R. Epp[1]*

[1]Department of Cell Biology and Anatomy, Hotchkiss Brain Institute, Cumming School of Medicine, University of Calgary, 3330 Hospital Drive NW, Calgary, Alberta, Canada T2N 4N1.

* Corresponding author

Dept. of Cell Biology & Anatomy

University of Calgary

HMRB 162, Health Sciences Centre

3330 Hospital Dr. NW

Calgary, AB

T2N 4N1

jonathan.epp1@ucalgary.ca

Pages: 21; # Figures: 4

Conflict of Interest Statement

The authors declare no conflicts of interest.

Acknowledgements

Funding for this study was provided by an NSERC Discovery Grant (RGPIN-2018-05135) to JRE. GAS received funding from NSERC, the Hotchkiss Brain Institute and the Cumming School of Medicine.

Abstract

Hippocampal neurogenesis has a role in many essential learning and memory processes, including forgetting. This forgetting process is important because it prevents proactive interference between old and new memories. While several studies have now established the role of neurogenesis in forgetting, the specific mechanisms mediating neurogenesis-induced forgetting have not been elucidated. The goal of this study was to examine how increased neurogenesis affects the recall of context fear memory in addition to its effects on population activity within hippocampal subregions. We trained mice in contextual fear conditioning and then increased neurogenesis via 4 weeks of voluntary wheel running. Increased neurogenesis led to a reduction in freezing behaviour during context testing, replicating previous studies showing that increased neurogenesis causes forgetting of context fear memories. Additionally, we mapped the expression of the immediate early gene c-Fos within hippocampal subregions and found that increasing neurogenesis led to reduced CA1 c-Fos expression during context testing. The results suggest that reduced CA1 population activity may underlie the association between increased neurogenesis and forgetting.

Introduction

Hippocampal neurogenesis is critical in the formation of long-term memories (Snyder et al. 2005; Wojtowicz, Askew, and Winocur 2008; Van Praag et al. 1999; Arruda-Carvalho et al. 2014). However, recent research on the retrograde effects of neurogenesis on long-term memory has found that increasing neurogenesis following learning causes forgetting of previously acquired memories (Akers et al. 2014; Epp et al. 2016; Cuartero et al. 2019; Ishikawa et al. 2016; Gao et al. 2018). This effect appears to impact a wide variety of memory types, occurs regardless of how neurogenesis levels are modulated, and appears to serve the purpose of mitigating the effects of proactive interference (Epp et al. 2016).

It is not clear exactly how neurogenesis modulates the hippocampal circuitry during memory recall to have this effect. However, it has been suggested that this effect might be mediated by the reconfiguration of intrahippocampal circuits as newly born DG cells form connections with CA3 neurons, leading to a failure to reactivate the original memory trace (Frankland, Köhler, and Josselyn 2013). Ablation of neurogenesis impairs the reactivation of engram cells in the CA3 during fear recall (Denny et al. 2014), showing that newly born DG cells have a significant effect on the activity of the CA3 during memory retrieval. Thus, a large increase in the number of new DG cells could also alter or disrupt the activity of CA3 engram cells. Moreover, these effects could extend further downstream to the CA1, especially given the extremely dense connectivity of CA1-CA1 relative to the more sparse DG-CA3 connectivity (Amaral, Ishizuka, and Claiborne 1990; Amaral 1993; Barnes et al. 1990).

One way to evaluate the effects of neurogenesis on hippocampal circuitry is the mapping of experience-dependent immediate early gene (IEG) expression, a technique that has previously been used extensively to identify the functions of hippocampal subregions and their activation by

memory encoding or retrieval (Kubik, Miyashita, and Guzowski 2007). In particular, the IEG c-Fos can be used as an endogenous marker for neurons that have recently undergone high frequency activity (Dragunow and Robertson 1987). Neurogenesis-induced intrahippocampal circuit alterations, and the resultant failure to retrieve memories, may be accompanied by altered levels of c-Fos expression, indicating altered levels of neuronal activity during memory retrieval.

In this experiment, we sought to identify whether neurogenesis-induced forgetting is associated with altered levels of neuronal activity in the hippocampus. Furthermore, we were interested in whether activity in individual subregions of the hippocampus would be differentially affected. Mice were first trained in a contextual fear conditioning task and then neurogenesis was increased via voluntary running. One month later, mice were tested in the task to confirm that neurogenesis promotes forgetting. Mice were then perfused 90 minutes later to quantify peak c-Fos expression in cells which were active at the time of the contextual memory test.

Methods & Materials

Subjects

Subjects were 28 female C57/B6 mice 60 days old at the start of the experiment. Mice were housed in standard cages with two to five mice per cage and free access to standard food and water *ad libitum*. The room lighting was maintained on a 12 hr /12 hr light/dark cycle (8 am, lights on), with contextual fear testing conducted during the light cycle phase. Experiments were conducted in accordance with the policies and guidelines of the Canadian Council on Animal Care Guidelines and the University of Calgary.

Manipulation of Neurogenesis

To increase neurogenesis, mice were given voluntary access to a saucer running wheel (Fast Trac™, Med Associates Inc., Fairfax, VT, United States, 16 cm in diameter) in their home cage for one month. Voluntary running is a highly reproducible and widely used approach to increase adult neurogenesis. It was chosen here because it has been used in previous experiments examining neurogenesis-induced forgetting where the behavioural effects were found to be specifically dependent on the increase in neurogenesis (Akers et al., 2014; Epp et al., 2016; Gao et al., 2018). Mice were trained to use running wheels by gently placing them on the running wheel and obstructing their path. Mice were considered trained if they ran on the wheel for approximately 30 seconds. Wheel revolutions were recorded continuously using the Wheel Manager software program (Med Associates Inc., Fairfax, VT, United States) and the number of wheel rotations was divided by the number of mice in the cage to give an estimated running distance per mouse. Mice in the sedentary group were housed conventionally with no running wheel but had standard enrichment items (dome house and nesting material).

Behavioural Testing

A schematic of the behavioural apparatus and experimental timeline used for CFC is shown in Figure 2A. Prior to contextual fear conditioning, all mice were handled for five minutes each day for three to five days until mice were calm with the handler. The Ugo Basile (Gemonio, Italy) contextual fear conditioning chambers (17 cm x 17 cm x 24.7 cm) were placed in noise reducing cabinets. The conditioning environment had shock grid floors (bars spaced 0.5 cm apart, 0.2 cm in diameter). Behaviour was monitored using overhead cameras and scored automatically using automated tracking software (ANY-Maze, Stoelting, Wood Dale, IL, United States). During

training, mice were allowed to explore the chamber for two minutes before being delivered three shocks (1 mA, 2 s) each separated by an interval of 1 minute. Mice were removed from the conditioning chamber one minute after the last shock and placed back in their home cage undisturbed for 24 hours. Then, running wheels were introduced to half of the mice. After four weeks of manipulating neurogenesis, mice were tested in the contextual fear task for five minutes with no shocks. The running wheel was locked the day prior to behavioural testing to prevent a direct effect of exercise on activity levels during testing. Freezing was used as the primary measure of memory retention and was defined as a complete lack of motion, except for respiration, for at least one second. Freezing was automatically calculated by the ANY-maze software system and was spot-checked for accuracy by an experimenter blind to treatment conditions.

Perfusions & Sectioning

Ninety minutes following the completion of the contextual conditioning task, mice were deeply anesthetized with isofluorane and then transcardially perfused with 0.1 M PBS and 4% formaldehyde. Brains were extracted and postfixed in 4% formaldehyde at 4°C for 24 hours. Brains were then cryoprotected with 30% sucrose in 0.1 M phosphate buffer at 4°C for three to five days until they sank. Brains were horizontally sectioned 40 µm thick on a cryostat (Leica CM 1950, Concord, ON, Canada) in 12 series. Sections were kept in a buffered antifreeze solution containing 30% ethylene glycol, and 20% glycerol in 0.1M PBS and stored at -20°C.

Immunohistochemistry

<u>Doublecortin labeling.</u> Tissue sections were washed three times in 0.1 M PBS at room temperature for ten minutes each. Sections were then transferred to a primary antibody solution

containing 1:500 goat anti-DCX antibody (c-18, sc-8066, Santa Cruz Biotechnology, Dallas, Texas, United States), 4% normal donkey serum, 0.4% Triton X, and 0.1 M PBS for 48 h. Sections then underwent three washes in 0.1 M PBS for ten minutes before being incubated for 24 h in a secondary antibody solution containing 1:500 Alexa Fluor 488 antibody (donkey anti-goat, CLAS10-1116, CedarLane Labs, Burlington, ON, Canada) and 0.1 M PBS. Finally, sections were incubated with 1:5000 DAPI and 0.1 M PBS for 20 minutes and then washed twice in 0.1 M PBS for ten mins per wash. For each wash step, primary/secondary antibody solution, or DAPI incubation, the tissue was gently oscillated at room temperature. Sections were then mounted on glass slides and coverslipped with No. 1.5H coverslips using PVA-DABCO mounting medium.

c-Fos labeling. Tissue sections were washed three times in 0.1 M PBS and then transferred to a primary antibody solution containing 1:500 rabbit anti-c-Fos antibody (226003, Synaptic Systems, Gottingen, Germany), 4% normal donkey serum, 0.4% Triton X, and 0.1 M PBS for 48 h. Tissue sections were then washed in 0.1 M PBS three times for ten minutes before being transferred to a secondary antibody solution for 24 h. Secondary antibody solution contained 1:500 Alexa Fluor 488 antibody (goat anti-rabbit, 4412S, Cell Signaling Technologies, Danvers, MA, United States; donkey anti-rabbit, 111-545-003, Cedarlane Labs, Burlington, ON, Canada; or donkey anti-rabbit, CLAS-12-2329, CedarLane Labs, Burlington, ON, Canada) with 0.1 M PBS. Finally, brain sections were incubated with 1:5000 DAPI and then washed twice in 0.1 M PBS. For each wash step, primary/secondary antibody solution, or DAPI incubation, the tissue was gently oscillated at room temperature. Sections were then mounted and coversliped with PVA-DABCO mounting medium.

Doublecortin Quantification

DCX labelled cells were counted in the granular and SGZ of the dentate gyrus of the hippocampus. Cells were counted if the cell was circular or ovular and the cell body could be clearly distinguished. Cells with a granular cytoplasmic pattern of fluorescence were excluded. To quantify the area of the DG, DAPI was imaged using a 405 nm laser set to 0.3% laser power, GaAsP detector sensitivity to 622V, gain at 1X, and offset set to 3%. Scan speed was set to 2 µs/pixel and scan size set to 1024x1024 pixels. Aperture was set to 8 Airy units. Images were acquired at 20X magnification and 2X optical zoom. The area of the granular zone in pixels was calculated using FIJI and converted to mm^2.

Automated c-Fos Quantification Pipeline

Image Acquisition. c-Fos labeled tissue was imaged using an Olympus FV3000 confocal microscope. All acquisition settings were kept constant across images. The 488nm laser power was set at 0.5%, GaAsP detector sensitivity at 492V, gain at 1X and offset at 3%. DAPI was imaged using a 405 nm laser set to 0.08% laser power, GaAsP detector sensitivity to 622V, gain of 1X and offset of 3%. Scan speed was set to 2 µs/pixel and scan size set to 1024x1024 pixels. Images were acquired with a 10X objective and 2X optical zoom (total magnification of 20X), with the aperture set to 1 Airy unit. Z-stacks step size was 3.64 µm. Images were separated into DAPI and c-Fos channels and then maximum intensity projected as a 2D image using FIJI software program.

c-Fos Quantification. Photomicrographs of c-Fos+ cells were segmented and converted to a binary image using the machine learning program Ilastik and quantified using FIJI. Images were

imported to Ilastik and underwent three steps to allow the program to selectively identify cell from background: training, object recognition, and regions of interest (ROI) testing (Figure 3A).

Ilastik Training and Object Recognition. First, a training set of images which were representative of the experimental images were imported to Ilastik which was then trained to distinguish signal from background. This set of training images allowed Ilastik to classify cell from background based on pixel features such as pixel intensity, edge features, and texture. With object recognition, Ilastik takes the trained image and generates a prediction of cell versus background based on object size, shape, and intensity.

Validation of Quantification by Ilastik. Following object recognition, sample ROIs from 12 mice (five sedentary, seven running) from the DG, CA3 and CA1 region were uploaded to Ilastik to test the program. To compare the Ilastik-generated cell counts to "ground truth" values, the ROIs were also counted manually by four independent researchers who were experienced with quantifying c-Fos but were blind to the Ilastik-generated counts as well as to the counts of the other experimenters. The cell counts were summed for each region and then compared to Ilastik-generated counts.

Batch Processing. Once Ilastik was adequately trained, the remaining c-Fos images were batch processed. The binary images were then imported to FIJI and overlaid with the DAPI image. Cells were then quantified using the binary image and area measured using FIJI. Area was then converted to mm^2. Cells were quantified by histological identification of the cellular layer of the DG, CA3 and CA1 region, with diffuse large cells used to identify the CA3 region and small, densely packed cells to identify the CA1 region.

Statistical Analysis

Hypothesis testing for behaviour, neurogenesis quantification, and c-Fos quantification were completed using GraphPad Prism 8. Independent t-tests were performed for DCX counts and behaviour. Running wheel data was binned to 1 week blocks of mean km/day/cage and analyzed using a 1-way repeated measures ANOVA. For c-Fos analysis, a two-way ANOVA was performed with Neurogenesis and Subregion as factors and Newman-Keuls post hoc tests were performed where appropriate. Grubbs' analysis was utilized to identify any potential outliers in the Ilastik validation data.

Hypothesis testing was complemented by estimation statistics for behaviour, neurogenesis quantification, and c-Fos quantification using estimationstats.com (Ho et al., 2019). Estimation statistics augment hypothesis testing by allowing a quantitative judgement about the relative magnitudes of effects rather than simple binary decisions related to statistical significance. Two group analyses were used for behaviour and DCX counts and a multiple two-group analysis was used for c-Fos expression. For each two-group comparison, effect size (Cohen's d) is calculated using a bootstrap sampling distribution using 5000 resamples along with a 95.0% confidence interval (CI; bias-corrected and accelerated). The data are plotted using estimation plots (Gardner-Altman plot for two-group analysis; Cumming plot for multiple two-group analysis) which show individual data points and the effect size of the comparisons. Comparisons that are deemed statistically significant via hypothesis testing are also marked on the plots.

Results

Voluntary Running Increases Neurogenesis

Representative photomicrographs of DCX+ cells in the DG are shown in Figure 1A. We found that running caused a significant increase in the number of DCX+ cells (Figure 1B. $t(26) = 3.57$, $p = 0.0014$; Cohen's $d = 1.35$ (95.0% CI 0.52, 2.07). In the running condition, mice ran approximately 3-5.5 km/day per mouse and this amount increased over successive weeks of running (Figure 1C. $F(3,15) = 17.34$, $p = 0.0193$).

Increasing Neurogenesis Following Learning Decreases Contextual Fear Memory Retrieval

During the training phase of the experiment, there was no significant difference in percent freezing between runners and sedentary controls (Figure 2B. $t(26) = 1.509$, $p = 0.1434$; Cohen's $d = -0.57$ (95.0% CI -1.36, 0.27)). After the running period, runners exhibited significantly lower Freezing than sedentary controls, consistent with decreased contextual fear memory (Figure 2C. $t(26) = 3.995$, $p = 0.0005$; Cohen's $d = -1.51$ (95.0% CI -2.62, -0.56)).

Validation of c-Fos Quantification Using Machine Learning

The cell counts produced using Ilastik fall within the 95% confidence intervals of the manually collected data set in all three subregions (Figure 3B). Ilastik performed at greater than or equal to 90% correspondence to the average of the manual cell counts in each hippocampal subregion (99.7% accuracy in DG, 97.7% accuracy in CA3 and 90.4% accuracy in CA1). The Ilastik cell count in CA1 was further from the mean of the manual counts compared to DG and CA1. However, this was clearly driven by an outlier in the manual counts. A Grubbs' analysis with alpha set to a conservative value of 0.01 identified this data point as an outlier. In the absence of this point, the Ilastik count was within 95% of the manual data points in CA1.

Increasing Neurogenesis Decreases CA1 c-Fos Expression During Recall

Representative photomicrographs of c-Fos+ cells in each of the hippocampal subregions is shown in Figure 4A. Expression of c-Fos differed by group and hippocampal subregion (Figure 4B. Significant interaction of Group × Subregion: $F(2,72) = 4.768$, $p = 0.0114$). The number of c-Fos positive cells was lower in runners than sedentary controls (Figure 4B. Significant main effect of Group: $F(1,72) = 4.602$, $p = 0.0353$), but examination of the effect sizes in each subregion reveals that c-Fos expression is essentially unchanged in the DG (Cohen's d = 0.32 (95.0% CI -0.52, 0.98)), with a slight reduction in c-Fos emerging in the CA3 (Cohen's d = -1.03 (95.0% CI -2.02, -0.06)) and growing largest in the CA1 (Cohen's d = -1.41 (95.0% CI -2.19, -0.41)). Post hoc tests revealed that the difference only reaches statistical significance in the CA1 ($p = 0.0214$), with no significant differences in the DG ($p = 0.884$) or the CA3 ($p = 0.6243$). These results indicate that increased neurogenesis causes a reduction in c-Fos expression that grows in magnitude further downstream of the DG, becoming largest in the CA1.

Discussion

In the present experiment, we sought to examine the mechanisms underlying neurogenesis-induced forgetting by identifying changes in experience-dependent c-Fos expression in the HPC associated with forgetting. We found that increasing neurogenesis caused forgetting of context fear memory and that this forgetting was associated with reduced c-Fos expression specifically within the CA1 subfield. The results replicate previous findings of neurogenesis-induced

forgetting in addition to extending this evidence by providing a potential mechanism by which neurogenesis reduces hippocampal memory expression.

Neurogenesis was robustly increased by voluntary running (van Praag et al., 1999a; van Praag et al., 1999b; Van Der Borght et al., 2007; Clark et al., 2008; Farmer et al., 2004; Kohman et al., 2012; Li et al., 2013; Akers et al., 2014; Epp et al., 2016). We found that one month of running resulted in an approximate doubling of neurogenesis similar to previous research (Akers et al., 2011; Epp et al., 2016). Moreover, increasing neurogenesis caused forgetting of a context fear memory, replicating previous reports (Akers et al. 2014; Ishikawa et al. 2016; Gao et al. 2018; Cuartero et al. 2019).

When examining the effects of increased neurogenesis on neuronal activity within the HPC via mapping of c-Fos expression, we found that increasing neurogenesis reduced c-Fos within the CA1. The CA1 has been shown to be active during recall of context fear memories (Hall, Thomas, and Everitt 2001; Jimenez et al. 2020) and impairments in fear memory recall can be induced though optogenetic disruption of the CA1 (Iwasaki and Ikegaya 2021; Goshen et al. 2011). A straightforward interpretation of our results is therefore that increasing neurogenesis reduces activity in the CA1 and impairs context fear memory recall as a consequence.

One explanation as to why we see this reduction in CA1 c-Fos expression after increasing neurogenesis is that the integration of new neurons into the hippocampal circuitry modulates excitatory transmission. Previous research has found that new neurons in the DG preferentially incorporate with hilar interneurons and CA3 interneurons (Restivo et al. 2015). Thus, increased neurogenesis in our running group could have resulted in a shift toward more inhibitory drive from the DG onto the CA3, resulting in decreased c-Fos expression downstream of the DG. An explanation for why this effect appears largest in the CA1 may be that DG-CA3 connections are

rather sparse compared with CA3-CA1 connections (David G. Amaral, Ishizuka, and Claiborne 1990; D. G. Amaral 1993; Barnes et al. 1990), meaning in theory that a small change in population activity in the CA3 could have amplified downstream effects in the CA1.

Another possibility is that increasing neurogenesis decreases mature granule neuron connectivity with the hippocampal circuitry. As neurogenesis increases, new synaptic connections preferentially form at the site of pre-existing synaptic boutons (Toni et al. 2007; Murray et al. 2020). Initially, axon terminals from both prenatal and adult-generated neurons synapse with these boutons, with a greater number of synapses associated with multiple synaptic bouton connections (MSBs) compared to single synaptic bouton connections (SSBs) (Toni et al. 2007). With time, the ratio of MSBs to SSBs is shifted, as a greater number of adult generated neurons associate with SSBs. One explanation for this is that adult-generated neurons primarily associate with MSBs and with time they out-compete prenatally generated neurons to form SSBs (Toni et al. 2007, 2008; Murray et al. 2020). Thus, if prenatally generated neurons active at the time of learning have reduced synaptic connectivity, this will result in fewer CA3 cells being activated during memory retrieval, as they are no longer innervated by granule cells active at the time of acquisition.

Importantly, the present experimental design does not rule out that reduced activity in the CA1 could be caused by some other effect of running which is neurogenesis-independent. Future experiments will be required to block neurogenesis during running or use pharmacological methods of increasing neurogenesis. Additionally, the c-Fos expression in our experiment reflects activity induced during fear memory recall, and additional experiments would be required to determine whether the reduced c-Fos in runners reflects a failure to activate the CA1 specifically during recall or if runners simply had lower baseline CA1 population activity.

In conclusion, we found that increasing neurogenesis via voluntary running caused forgetting of a context fear memory. Additionally, this forgetting effect was associated with reduced c-Fos expression in the CA1, indicating reduced CA1 population activity during recall. The results suggest that reduced CA1 activation could be a mechanism mediating neurogenesis-induced forgetting. Increased neurogenesis may reduce CA1 population activity through increased inhibitory drive of the DG onto downstream hippocampal subregions or through the displacement of existing synapses formed by mature granule cells.

References

Akers, Katherine G., Alonso Martinez-canabal, Leonardo Restivo, Adelaide P. Yiu, Antonietta De Cristofaro, Hwa-Lin (liz) Hsiang, Anne L. Wheeler, et al. 2014. "Hippocampal Neurogenesis Regulates Forgetting during Adulthood and Infancy." *Science* 598 (May): 598–603.

Amaral, David G., Norio Ishizuka, and Brenda Claiborne. 1990. "Chapter 1. Neurons, Numbers and the Hippocampal Network." In *Progress in Brain Research*, edited by J. Storm-Mathisen, J. Zimmer, and O. P. Ottersen, 83:1–11. Elsevier.

Amaral, David G. 1993. "Emerging Principles of Intrinsic Hippocampal Organization." *Current Opinion in Neurobiology* 3 (2): 225–29.

Arruda-Carvalho, Maithe, Leonardo Restivo, Axel Guskjolen, Jonathan R. Epp, Ype Elgersma, Sheena A. Josselyn, and Paul W. Frankland. 2014. "Conditional Deletion of α-CaMKII Impairs Integration of Adult-Generated Granule Cells into Dentate Gyrus Circuits and Hippocampus-Dependent Learning." *The Journal of Neuroscience: The Official Journal of the Society for Neuroscience* 34 (36): 11919–28.

Barnes, Carol A., Bruce L. McNaughton, Shed J. Y. Mizumori, Brian W. Leonard, and Lei-Huey Lin. 1990. "Chapter 21. Comparison of Spatial and Temporal Characteristics of Neuronal Activity in Sequential Stages of Hippocampal Processing." In *Progress in Brain Research*, edited by J. Storm-Mathisen, J. Zimmer, and O. P. Ottersen, 83:287–300. Elsevier.

Cuartero, María Isabel, Juan de la Parra, Alberto Pérez-Ruiz, Isabel Bravo-Ferrer, Violeta Durán-Laforet, Alicia García-Culebras, Juan Manuel García-Segura, et al. 2019. "Abolition of Aberrant Neurogenesis Ameliorates Cognitive Impairment after Stroke in Mice." *The Journal of Clinical Investigation* 129 (4): 1536–50.

Denny, Christine A., Mazen A. Kheirbek, Eva L. Alba, Kenji F. Tanaka, Rebecca A. Brachman, Kimberly B. Laughman, Nicole K. Tomm, Gergely F. Turi, Attila Losonczy, and René Hen. 2014. "Hippocampal Memory Traces Are Differentially Modulated by Experience, Time, and Adult Neurogenesis." *Neuron* 83 (1): 189–201.

Dragunow, M., and H. A. Robertson. 1987. "Kindling Stimulation Induces c-Fos Protein(s) in Granule Cells of the Rat Dentate Gyrus." *Nature* 329 (6138): 441–42.

Epp, Jonathan Richard, Rudy Silva Mera, Stefan Kohler, Sheena A. Josselyn, and Paul W. Frankland. 2016. "Neurogenesis-Mediated Forgetting Minimizes Proactive Interference." *Nature Communications* 7 (10838): 5–12.

Frankland, Paul W., Stefan Köhler, and Sheena A. Josselyn. 2013. "Hippocampal Neurogenesis and Forgetting." *Trends in Neurosciences* 36 (9): 497–503.

Gao, Aijing, Frances Xia, Axel J. Guskjolen, Adam I. Ramsaran, Adam Santoro, Sheena A. Josselyn, and Paul W. Frankland. 2018. "Elevation of Hippocampal Neurogenesis Induces a Temporally Graded Pattern of Forgetting of Contextual Fear Memories." *Journal of Neuroscience* 38 (13): 3190–98.

Goshen, Inbal, Matthew Brodsky, Rohit Prakash, Jenelle Wallace, Viviana Gradinaru, Charu Ramakrishnan, and Karl Deisseroth. 2011. "Dynamics of Retrieval Strategies for Remote Memories." *Cell* 147 (3): 678–89.

Hall, Jeremy, Kerrie L. Thomas, and Barry J. Everitt. 2001. "Cellular Imaging of zif268 Expression in the Hippocampus and Amygdala during Contextual and Cued Fear Memory Retrieval: Selective Activation of Hippocampal CA1 Neurons during the Recall of Contextual Memories." *The Journal of Neuroscience: The Official Journal of the Society*

for Neuroscience 21 (6): 2186–93.
Ishikawa, Rie, Hotaka Fukushima, Paul W. Frankland, and Satoshi Kida. 2016. "Hippocampal Neurogenesis Enhancers Promote Forgetting of Remote Fear Memory after Hippocampal Reactivation by Retrieval." *eLife* 5 (September): 1–17.
Iwasaki, Satoshi, and Yuji Ikegaya. 2021. "Contextual Fear Memory Retrieval Is Vulnerable to Hippocampal Noise." *Cerebral Cortex* 31 (2): 785–94.
Jimenez, Jessica C., Jack E. Berry, Sean C. Lim, Samantha K. Ong, Mazen A. Kheirbek, and Rene Hen. 2020. "Contextual Fear Memory Retrieval by Correlated Ensembles of Ventral CA1 Neurons." *Nature Communications* 11 (1): 3492.
Kubik, Stepan, Teiko Miyashita, and John F. Guzowski. 2007. "Using Immediate-Early Genes to Map Hippocampal Subregional Functions." *Learning & Memory* 14 (11): 758–70.
Murray, Karl D., Xiao-Bo Liu, Anna N. King, Julie D. Luu, and Hwai-Jong Cheng. 2020. "Age-Related Changes in Synaptic Plasticity Associated with Mossy Fiber Terminal Integration during Adult Neurogenesis." *eNeuro* 7 (3). https://doi.org/10.1523/ENEURO.0030-20.2020.
Restivo, Leonardo, Yosuke Niibori, Valentina Mercaldo, Sheena A. Josselyn, and Paul W. Frankland. 2015. "Development of Adult-Generated Cell Connectivity with Excitatory and Inhibitory Cell Populations in the Hippocampus." *The Journal of Neuroscience: The Official Journal of the Society for Neuroscience* 35 (29): 10600–612.
Snyder, Jason S., N. S. Hong, Robert J. McDonald, and Jan Martin Wojtowicz. 2005. "A Role for Adult Neurogenesis in Spatial Long-Term Memory." *Neuroscience* 130 (4): 843–52.
Toni, Nicolas, Diego A. Laplagne, Chunmei Zhao, Gabriela Lombardi, Charles E. Ribak, Fred H. Gage, and Alejandro F. Schinder. 2008. "Neurons Born in the Adult Dentate Gyrus Form Functional Synapses with Target Cells." *Nature Neuroscience* 11 (8): 901–7.
Toni, Nicolas, E. Matthew Teng, Eric A. Bushong, James B. Aimone, Chunmei Zhao, Antonella Consiglio, Henriette van Praag, Maryann E. Martone, Mark H. Ellisman, and Fred H. Gage. 2007. "Synapse Formation on Neurons Born in the Adult Hippocampus." *Nature Neuroscience* 10 (6): 727–34.
Van Praag, Henriette, Brian R. Christie, Terrence J. Sejnowski, and Fred H. Gage. 1999. "Running Enhances Neurogenesis, Learning, and Long-Term Potentiation in Mice." *Proceedings of the National Academy of Sciences of the United States of America* 96 (23): 13427–31.
Wojtowicz, Jan Martin, Michele L. Askew, and Gordon Winocur. 2008. "The Effects of Running and of Inhibiting Adult Neurogenesis on Learning and Memory in Rats." *The European Journal of Neuroscience* 27 (6): 1494–1502.

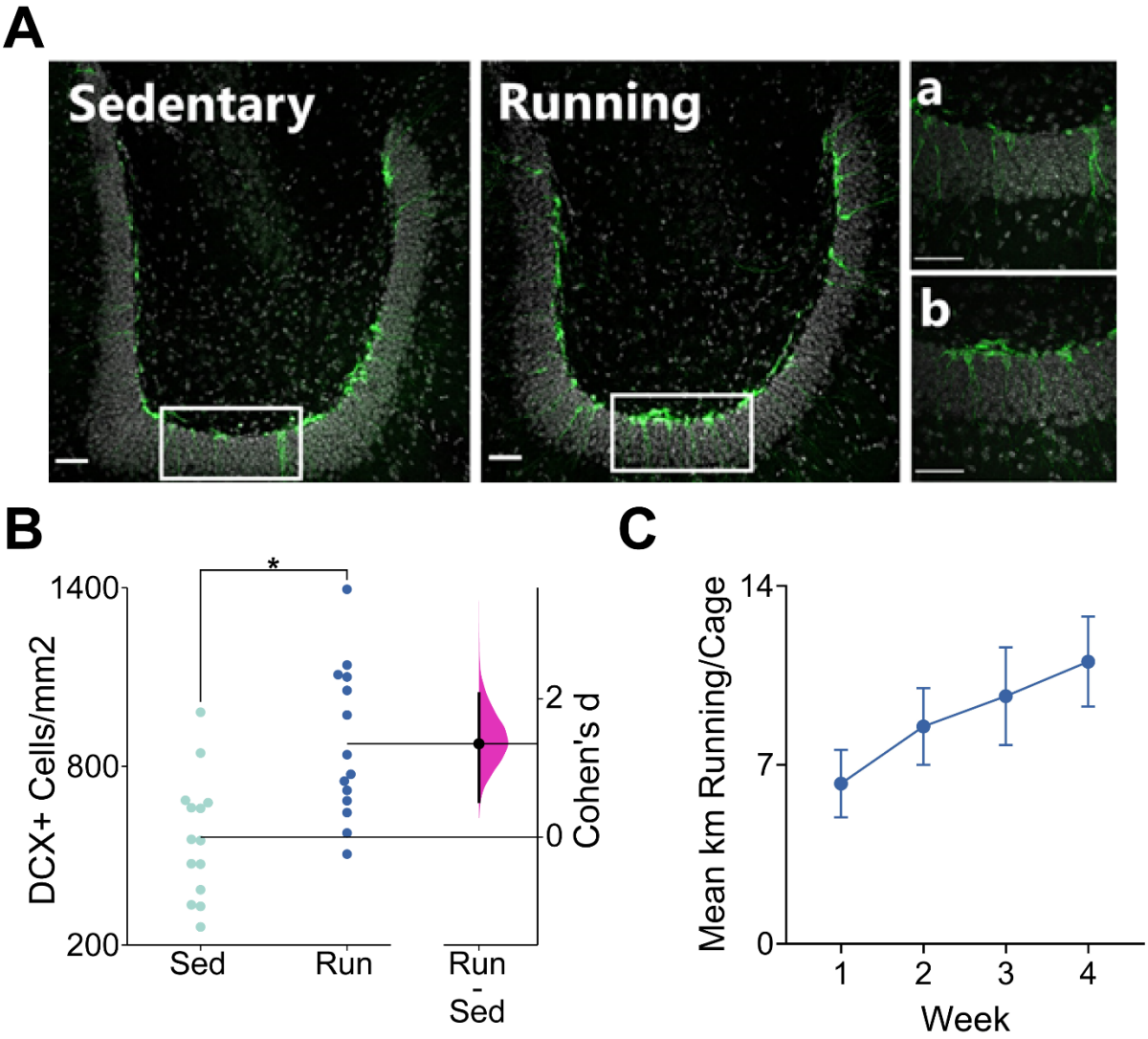

Figure 1. A) A photomicrograph of a ventral section of the apex of the DG for sedentary and running groups stained with DCX (green) and DAPI (grey). Inset a, apex of the DG representative of the sedentary controls; inset b, apex of the DG representative of the runners; scale bar, 50 µm. B) DCX+ cells/mm^2 in runners (Run) and sedentary controls (Sed). Data are shown as individual data points with mean (horizontal lines) and DCX+ cells/mm^2 scale on the left Y-axis. Effect size (Cohen's d) is shown as a black circle with vertical lines and gaussian distribution for the bootstrap 95% CI and Cohen's d scale on the right y-axis. DCX+ cells/mm^2 were significantly increased in runners. C) Mean (±SEM) km of running/day/week/cage. Individual mice completed ~3-5.5 of running per day (cage wheel count/2) and this amount significantly increased over successive weeks of running.

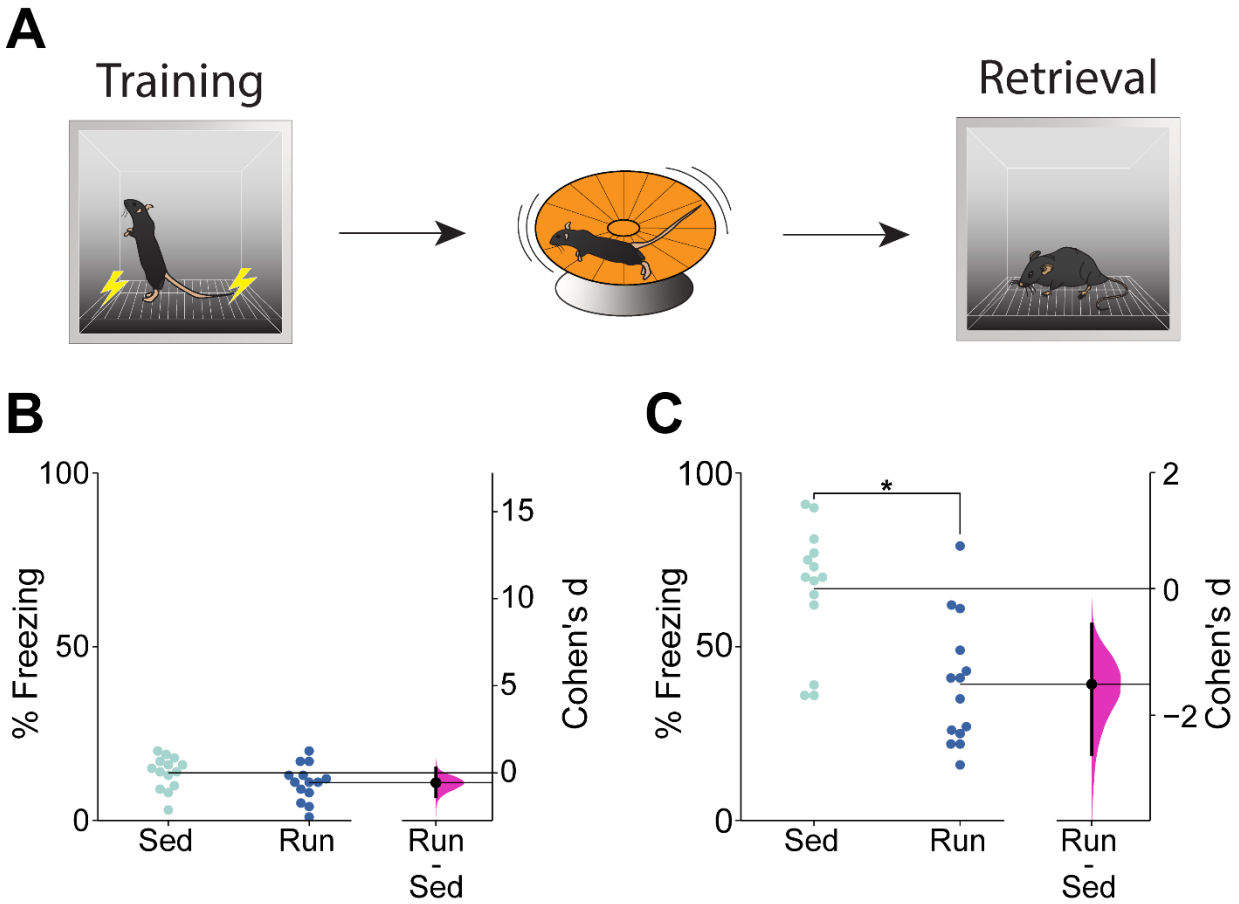

Figure 2. A) A schematic showing the behavioural apparatus and experimental timeline used for CFC. B) % Freezing during CFC training in runners (Run) and sedentary controls (Sed). Data are shown as individual data points with mean (horizontal lines) and % Freezing scale on the left Y-axis. Effect size (Cohen's d) is shown as a black circle with vertical lines and gaussian distribution for the bootstrap 95% CI and Cohen's d scale on the right y-axis. During training, there was no significant difference in % Freezing between groups. C) % Freezing during CFC testing after running or sedentary control. Data are shown as individual data points with mean (horizontal lines) and % Freezing scale on the left Y-axis. Effect size (Cohen's d) is shown as a black circle with vertical lines and gaussian distribution for the bootstrap 95% CI and Cohen's d scale on the right y-axis. Runners froze significantly less than sedentary controls, indicating forgetting of the fear memory after elevation of neurogenesis.

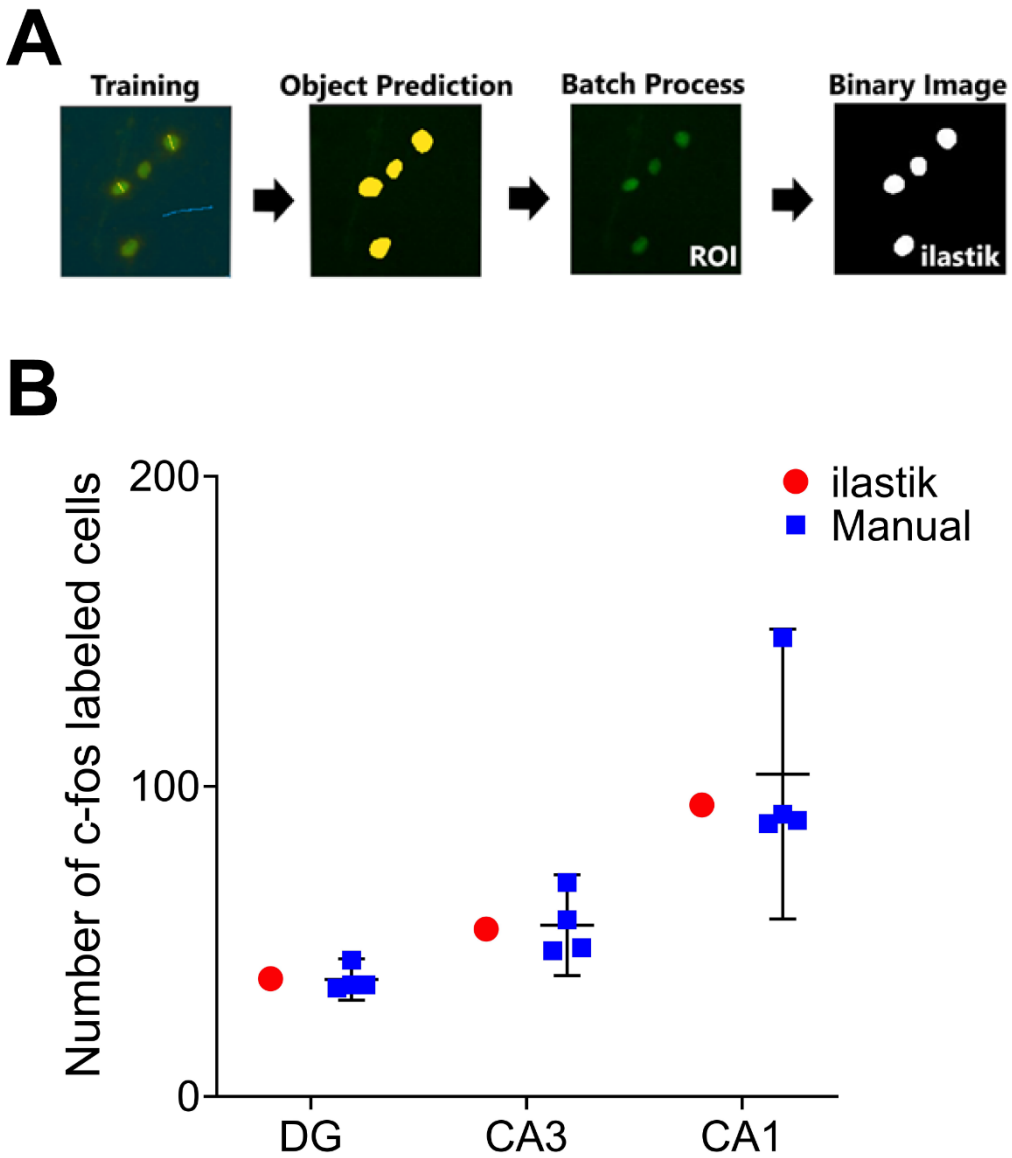

Figure 3. A) The protocol for c-Fos quantification using Ilastik. A max projected c-Fos image was used to train the program to identify cells from background. After Ilastik was trained, it generated object predictions of what it considered a "cell". The user then corrects for any incorrect predictions to allow the program to make predictions based on cell size, pixel intensity, and so forth. When the user considers the program sufficiently trained, the program is tested to compare manual counts with Ilastik counts. The program is considered sufficiently trained when Ilastik generates counts within 5% of manual counts. B) Comparison of Ilastik c-Fos estimates (red) versus manual c-Fos counts (blue). Horizontal bars represent sample mean of the manual counts. Error bars represent 95% confidence intervals. Ilastik-generated counts were comparable to that of manual counts for the DG, CA3, and CA1 regions.

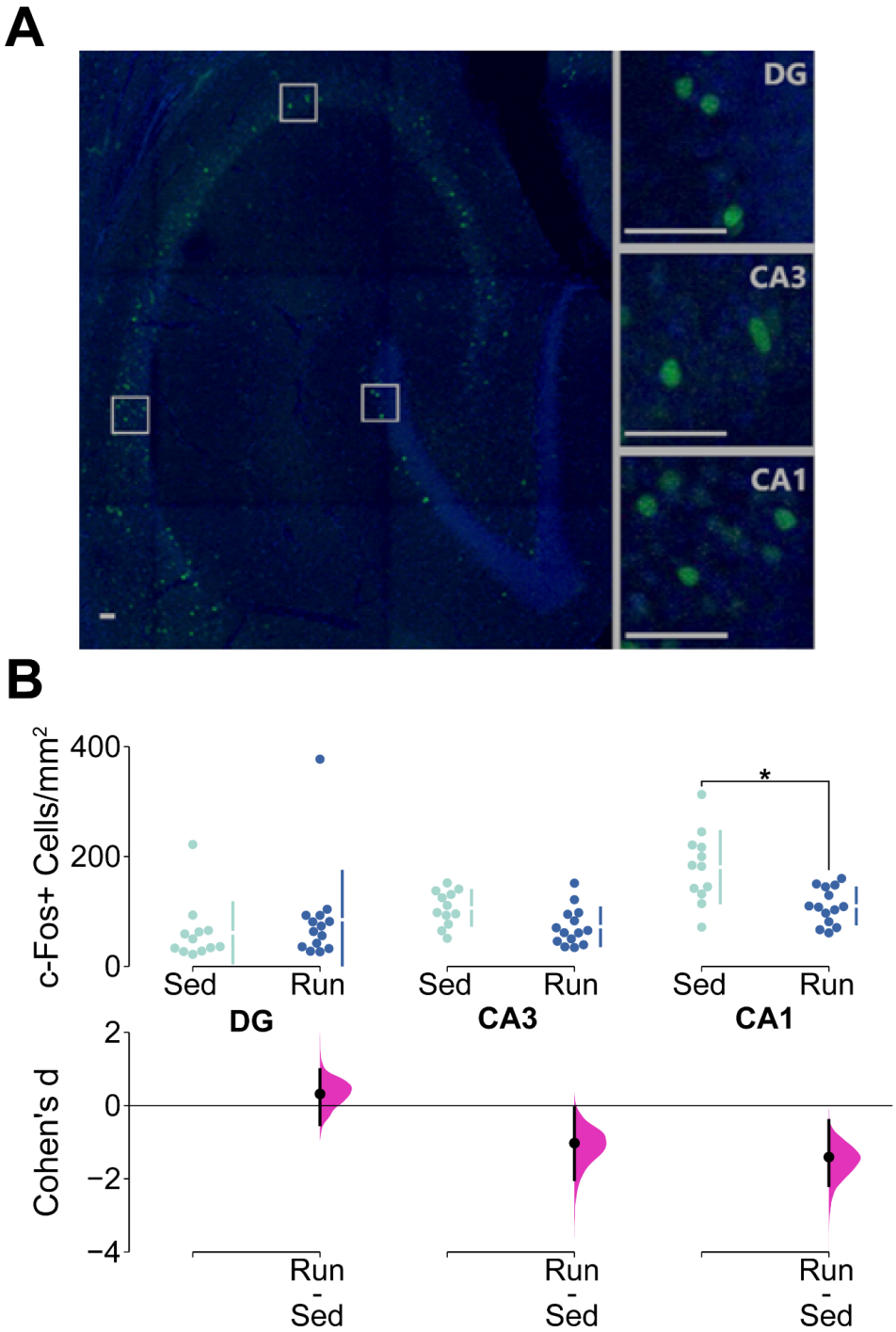

Figure 4. A) Photomicrograph of c-Fos staining in the Hippocampus. c-Fos stained cells (green) are clearly observable in DAPI stained tissue (blue) in the DG, CA3 region and CA1 region. Scale bar, 50 µm. B) c-Fos+ cells/mm^2 in runners (Run) and sedentary controls (Sed) within the DG, CA3, and CA1. Upper portion of the plot shows individual data points in swarm plots with means (±SD; gapped vertical line). Lower portion of the plot shows effect size (Cohen's d) as a black circle with vertical lines and gaussian distributions for the bootstrap 95% CI. Runners had significantly reduced c-Fos expression relative to sedentary controls specifically within the CA1.